

Metal-Insulator and Insulator-Insulator Transitions in the Quarter-Filled Band Organic Conductors

K. C. Ung, S. Mazumdar, and D. Toussaint

Department of Physics, University of Arizona, Tucson, Arizona 85721

(Received 25 April 1994)

The theory of the $2k_F$ and $4k_F$ instabilities in quarter-filled band organic conductors is revisited. The phase angles of the $2k_F$ bond and charge density waves change as electron correlation is turned on, and this switching of the phase angle is critical for understanding the bond distortion patterns in the real materials. Intersite Coulomb interactions in the real materials must be nonzero but less than a critical value. Both intersite and intrasite charge density waves are destabilized in the quasi-two-dimensional regime for realistic parameters, explaining the weakening of these phases in the superconducting materials.

PACS numbers: 71.28.+d, 71.30.+h, 71.45.Lr

Conducting organic charge-transfer solids are of interest as highly doped Mott-Hubbard semiconductors. Nearly forty of these materials are superconducting, and evidence exists for strong Coulomb interactions among the fermions in these systems [1]. For a complete understanding of their normal state, it is essential that the spatial broken symmetries in the quasi-one-dimensional (quasi-1D) nonsuperconducting conductors be understood. In addition to the usual $2k_F$ Peierls instability, many of the organic conductors exhibit a $4k_F$ instability (k_F is the one-electron Fermi wave vector) [2]. Despite considerable theoretical work, important issues involving distortions in the real materials and the parameter space in which the materials lie remain largely unresolved. This is primarily due to the limitations of calculations of susceptibilities [3–5] that do not measure actual distortion patterns or charge densities. We give here a detailed picture of the transitions in the actual experimental quasi-1D systems, that also has significant implications for the quasi-2D superconductors, where these transitions are absent or weakened.

We limit ourselves to $\rho = 0.5$, where ρ is the number of electrons per site. For this commensurate case, the bond order wave (BOW), with periodic modulation of the intersite distances, and the charge density wave (CDW), with modulation of the intrasite charge densities, are distinct. Each of these can have periodicities $2k_F$ (period 4) and $4k_F$ (period 2). Furthermore, each period 4 density wave can occur in two forms, corresponding to different phase angles. Table I shows the period 4 and period 2 patterns. For zero Coulomb interactions, the ground state consists of coexisting $2k_F$ BOW1 and CDW1 [6]. Table I also shows the observed bond distortion pattern [7] below the $2k_F$ transition in MEM(TCNQ)₂, where this pattern is precisely known. The bond distortion in semiconducting TEA(TCNQ)₂ [8] is identical and is accompanied by a modulation of intramolecular charge that resembles the $2k_F$ CDW2 of Table I [8].

Existing theories [3–5,9–11] do not explain several of the mysteries in the real materials. For example, the $4k_F$

phase has been interpreted as a CDW by various authors [9–11]. This would (qualitatively) imply occupancy of alternate sites by electrons (see Table I, row 2, column 3). Since the $4k_F$ and $2k_F$ CDWs do not coexist [4], for the $2k_F$ transition to occur on the same chain, the $2k_F$ phase must be a spin density wave (SDW) or a spin Peierls state. We discount the possibility of the SDW, as long range SDW is not possible in one dimension even at 0 K. The spin Peierls state that can accompany the $4k_F$ CDW is the BOW1 state of Table I, in which the distances between the “occupied” sites are alternating. The experimental bond tetramerized phase is, however, different from BOW1, and therefore we conclude that the $4k_F$ cannot be a CDW to begin with. The $4k_F$ phase can also be a BOW, and indeed in this case peaks in the wave-vector dependent charge-transfer susceptibility are found at both $2k_F$ and $4k_F$ within the extended Hubbard model [4]. What is still not clear is how the experimental bond distortion pattern is obtained below the $2k_F$ transition, as no combination of the $4k_F$ BOW and the $2k_F$ BOW1 (which

TABLE I. The possible bond distortions and charge modulations in a $\rho = 0.5$ chain. The single bonds correspond to undistorted bonds, while the double and dotted bonds correspond to short and long bonds, respectively. The last column gives the bond distortion pattern in MEM(TCNQ)₂ below the $2k_F$ transition. Here the double dotted bond is a long bond which is shorter than the single dotted bond. In the case of the CDWs, the lengths of the vertical bars on the sites correspond to the charge densities.

BOW and CDW patterns in $\rho=0.5$			
Period 4	Period 4	Period 2	MEM(TCNQ) ₂
$2k_F$ BOW1	$2k_F$ BOW2	$4k_F$ BOW	BOW
$2k_F$ CDW1	$2k_F$ CDW2	$4k_F$ CDW	CDW

dominates over the BOW2 for noninteracting electrons) can give the observed distortion pattern. The nature of the CDW that accompanies the $4k_F$ BOW in these commensurability >2 systems has not been investigated. Optical absorption in MEM(TCNQ)₂ below the $4k_F$ transition has previously been explained within a dimer model [12,13] which retains only two neighboring TCNQ molecules and assumes that a single electron occupies the dimer. This model assumes that the $4k_F$ phase is a BOW, but the nature of the CDW is ambiguous, as both the $4k_F$ CDW and the $2k_F$ CDW2 would satisfy the condition of "one" electron per dimer.

We show here that a clearer picture of the instabilities emerges if phonons are included explicitly in the calculations, and actual bond distortions and charge modulations are calculated. Our most significant findings are the following: (i) The phase angles of the lowest energy period 4 structures change with nonzero Coulomb interaction. This switching of the phase angles is central to the detailed understanding of the $4k_F$ and the $2k_F$ transitions. (ii) Exactly as the $2k_F$ BOW1 and $2k_F$ CDW1 coexist for all electron-molecular-vibration (e-mv) and electron-intersite-phonon (e-ph) couplings [6], the $2k_F$ BOW2 and the $2k_F$ CDW2 also coexist. (iii) For the intersite Coulomb interaction nonzero but less than a critical value, the ground state has a $4k_F$ BOW component in addition to the $2k_F$ BOW2 and CDW2 components. The experimental lowest energy bond distortion pattern now emerges naturally as a combination of the period 2 BOW and the period 4 BOW2.

The Hamiltonian we consider is

$$\begin{aligned}
 H = & \sum_{i\sigma} [t - \alpha(u_{i+1} - u_i)] (c_{i\sigma}^\dagger c_{i+1,\sigma} + c_{i+1,\sigma}^\dagger c_{i\sigma}) \\
 & + U \sum_i n_{i\uparrow} n_{i\downarrow} + V \sum_i n_i n_{i+1} \\
 & + \frac{K_1}{2} \sum_i (u_{i+1} - u_i)^2 \\
 & + \beta \sum_i n_i v_i + \frac{K_2}{2} \sum_i v_i^2.
 \end{aligned} \quad (1)$$

Here $c_{i\sigma}^\dagger$ creates an electron of spin σ at site i , $n_{i\sigma} = c_{i\sigma}^\dagger c_{i\sigma}$, $n_i = \sum_\sigma n_{i\sigma}$, t is the one-electron hopping integral, and U and V are the on-site and nearest neighbor Coulomb repulsions. The u_i are the displacements of the i th molecular units from their equilibrium positions, v_i correspond to an internal molecular mode, α and β are the e-ph and e-mv coupling constants, and K_1 and K_2 are the corresponding elastic constants.

Exact calculations were done for rings of 8, 12, and 16 sites, both with and without the restriction of fixed overall ring size. We first show the results for fixed overall size. We initially assume $\beta = 0$ and $u_j = u_0 \cos(2k_F j - \theta)$. The calculations are done for periodic $N = 8$ and 12, with both $\theta = 0$ and $\theta = \pi/4$, corresponding to the

BOW1 and BOW2, respectively. The $N = 8$ periodic ring with 4 electrons distorts spontaneously for even small $\lambda = \alpha^2/Kt$, while the $N = 12$ with 6 electrons requires a much larger λ . This is a well known difference between finite periodic $4n$ and $4n + 2$ electron systems which at $U = 0$ have degenerate and nondegenerate ground states, respectively. The $2k_F$ BOW is weakened by U in both cases. However, the more significant result is the crossover from $\theta = 0$ to $\theta = \pi/4$, as shown in Fig. 1(a), corresponding to a transition from $2k_F$ BOW1 to $2k_F$ BOW2 for nonzero U . The crossing occurs at a much larger U for $N = 12$ than for $N = 8$. This is expected, as the larger λ needed to induce the distortion in the $N = 12$ also increases the energy difference between BOW1 and the BOW2 at $U = 0$. The minimum λ at which the $4n + 2$ electron periodic rings distort decreases with increasing size [6], and therefore the critical U at which the energy crossing occurs in the $N = 12$ is an upper bound for the infinite chain at small λ .

In addition to changing θ , Coulomb interactions also add a $4k_F$ component. We repeat our calculations with the ansatz $u_j = u_0[r_2 \cos(2k_F j - \theta_2) + r_4 \cos(4k_F j - \theta_4)]$, $r_2 + r_4 = 1$. The absolute lowest energy within correlated models occurs for $\theta_2 = \pi/4$, $\theta_4 = 0$, and $r_4 \neq 0$. Furthermore, r_4 increases monotonically with U and for fixed U increases rapidly with V , provided V is less than a critical value $V_c(U)$. We discuss the issue of V_c below. The effects of U and V on r_4 are summarized in Fig. 1(b). Note that the calculated bond distortion pattern is identical to the experimentally observed distortion in MEM(TCNQ)₂ below the $2k_F$ transition and in TEA(TCNQ)₂ for $r_4 > 0.41$. The U at which r_4 exceeds 0.41 is different for $N = 8$ and $N = 12$, but this difference decreases rapidly with V [see Fig. 1(b)], indicating once again that the difference between $4n$

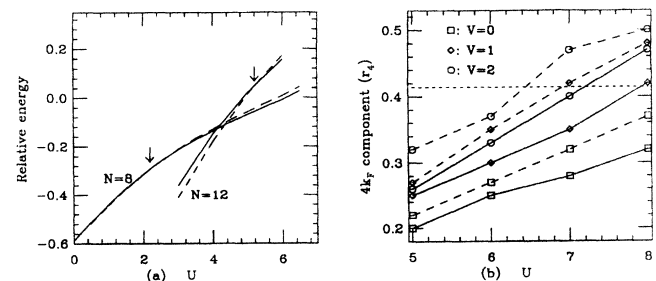


FIG. 1. (a) The gain in total energy vs U for $2k_F$ bond distortions for periodic $N = 8$ and 12. The calculations are for $\lambda = 0.8$ for $N = 8$ and 1.41 for $N = 12$ (see text). The solid line in each case corresponds to the BOW1 and the dashed line to the BOW2. The arrows indicate the crossing of the BOW1 and BOW2 energies. (b) The relative weight r_4 of the $4k_F$ component of the ground state wave function as a function of U and V . The dashed and solid curves correspond to $N = 8$ and 12, respectively. The values for λ are the same as in (a). For $r_4 > 0.41$ the bond distortion pattern is identical to that observed in MEM(TCNQ)₂ below the $2k_F$ transition.

and $4n + 2$ electron systems vanishes in the long chain limit. We conclude that the crossover in θ and nonzero $r_4 > 0.41$ are both necessary to explain the experimental bond distortion. Calculations of susceptibilities [3–5] do not distinguish between BOW1 and BOW2 and also cannot give the exact bond distortion pattern.

The issue of V_c can be understood as follows. In the limit of $U \rightarrow \infty$ and $\beta = 0$, Eq. (1) reduces to the half-filled band of spinless fermions with nearest neighbor interaction V . Within the spinless fermion Hamiltonian, transition to a $4k_F$ CDW with equal bond lengths occurs for $V > V_c = 2t$ and small λ . For $V < 2t$ a dimerized BOW appears for infinitesimal λ , with the bond dimerization increasing with V [14]. Numerical simulations in the limit of $\lambda = 0$ indicate that even for finite U , a CDW appears only above a $V_c(U)$, which is now slightly larger than $2t$ [15]. The increase of r_4 with V within Eq. (1) is then expected for $V < V_c(U)$. Thus the observed periodicity indicates that experimental materials are in the $V < V_c$ regime.

The above results were confirmed by a second set of calculations. Instead of using the size constraint and the ansatz for u_i , the ground state energy was minimized with respect to a position dependent $t_i = t + \alpha(u_{i+1} - u_i)$. Using a complete basis of electron configurations and an initial guess for the t_i , we used the Lanczos method to find the ground state. We evaluate $\delta E/\delta t_i$, adjust the t_i to decrease the energy (steepest descent), and repeat the process until the t_i converge. These calculations were done for $N = 8$ and 16 with periodic boundary conditions and $N = 12$ with antiperiodic boundary condition. The antiperiodic boundary condition for $N = 12$ introduces the same Fermi level degeneracy in the absence of the distortion that characterizes periodic $N = 8$ and 16, allowing calculations with the same λ in all cases. We again find that for $U = V = 0$ the BOW1 is lower in energy, but for nonzero U the BOW2 is favored.

As in the previous case, the absolute ground state is once again found to be a composite of the $4k_F$ BOW and the $2k_F$ BOW2. To display the distortion patterns we compute the Fourier transform $T(q)$ of the final hopping parameters t_i which minimize the energy. Period four distortions appear as a peak in the Fourier transform at momentum $2k_F$, and the difference between the BOW1 and the BOW2 patterns is the phase of this Fourier component. Similarly the period 2 component of the distortion appears at momentum $4k_F$. Crossover occurs from a dominant $2k_F$ to a dominant $4k_F$ when $T(4k_F) > T(2k_F)$. Our results are summarized in Figs. 2(a) and 2(b), where the $2k_F$ curves correspond to the lower energy BOW2 phase. As in Fig. 1(b), here also nonzero U enhances the $4k_F$ contribution to the wave function, but the $4k_F$ dominates the $2k_F$ only for nonzero moderate V . Once the $4k_F$ contribution dominates, the overall bond distortion pattern is exactly the same as that of MEM(TCNQ)₂ and TEA(TCNQ)₂.

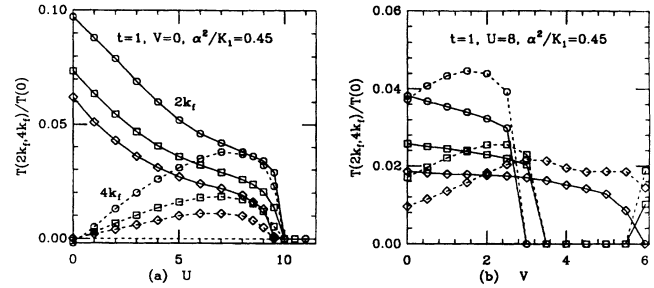


FIG. 2. The $2k_F$ (solid lines) and $4k_F$ (dashed lines) components of the hopping parameters t_i at $V = 0$ and $\lambda = \alpha^2/K_1 = 0.45$. (a) Results are shown for $N = 8$ (circles) and $N = 16$ (diamonds) with periodic boundary conditions (circles) and for $N = 12$ with antiperiodic boundary conditions (squares). In all cases we see that the $4k_F$ component increases with U until at very large U the distortion vanishes completely. Note that U alone is insufficient to drive the $4k_F$ component larger than the $2k_F$ component, which is the condition for the pattern to change from “medium-short-medium-long” to “short-medium-short-long.” (b) Same as (a) for fixed $U = 8$ and varying V . Note that V enhances the $4k_F$ component, which can now be larger than the $2k_F$ component. The results for $L = 16$ at large V may be an artifact of the small system size. At the end of this curve, at $V = 6$, the $L = 16$ distortion is purely $4k_F$, or period two. However, the wave function at this point has a period of four, changing sign under translation by two lattice sites. For the undistorted lattice, this corresponds to a ground state with nonzero momentum.

We also find that just as the BOW1 coexists with CDW1 [6], the BOW2, and the composite ground state of BOW2 and the $4k_F$ BOW, coexist with the CDW2. The CDW2 is confirmed by monitoring the actual site charge densities.

All of the above results can be physically understood within a real space approach to spatial broken symmetries that has been used to understand the half-filled band in one [16] and two [17] dimensions, as well as CDWs in 1D bands with arbitrary ρ [5]. In this approach, the behavior of density waves is understood from repeat units in appropriate many-electron configurations in real space. For example, the CDW in the half-filled band can be understood by examining the configuration ...2020..., where the numbers denote site occupancies by electrons. Since charge transfer from an atom to its left or right are exactly equal in the above configuration, we can infer that the CDW and the BOW do not coexist in $\rho = 1$. Similarly, double occupancies are destroyed by U , and therefore the Hubbard U should destroy the CDW. In $\rho = 0.5$, the only possible repeat units are site occupancies ...2000..., ...1100..., and ...1010.... The last configuration leads to the $4k_F$ CDW and is not of interest here. The $2k_F$ BOW1 that occurs at $U = 0$ is understood in terms of the repeat unit ...2000.... Large charge transfer between the “doubly occupied” site and the neighboring “empty sites” promotes two strong bonds, while weak charge transfer between neighboring empty sites promotes

two consecutive weak bonds. Similarly, we also expect a large charge density on the “doubly occupied” site, an intermediate charge density on the neighboring empty site, and an even weaker charge density on the next neighbor empty site, i.e., $2k_F$ CDW1. As U increases, the contribution of ...2000... to the wave function decreases while that of ...1100... increases (for small V). In high spin eigenstates, the configuration ...1100... would promote weak bonds between the two “occupied sites” and the two “unoccupied sites” and strong bonds between an occupied site and a neighboring unoccupied site. In low spin eigenstates, there are two different types of weak bonds, between singly occupied neighboring sites with opposite spins and between unoccupied sites. The latter distortion pattern agrees with that in the last column of Table I and must coexist with $2k_F$ CDW2. Thus the change in the phase angles of the $2k_F$ components of the BOW and the CDW found numerically can be anticipated from physical reasonings.

The above results give a complete picture of the $2k_F$ and $4k_F$ instabilities in the real materials. The free energy of the experimental system is dominated by high spin states at high temperatures, whose electronic behavior is similar to that of spinless fermions. For $V < V_c(U)$ the lattice dimerizes to the $4k_F$ BOW below the $4k_F$ transition temperature. At still lower temperatures, the free energy is dominated by low spin states, and the behavior now would resemble that of the ground state of Eq. (1). Dimerization of the dimerized lattice now takes place, and the overall bond distortion pattern resembles that in the last column of Table I. Coexistence of these states with the $2k_F$ CDW2 also explains the observed charge modulation pattern [8] in TEA(TCNQ)₂. For nonzero β , bond lengths within consecutive TCNQ molecules along the stack axis will reflect the CDW2.

Although we have focused on the quasi-1D nonsuperconductors, our results have implications for the quasi-2D superconducting TMTSF and the BEDT-TTF based materials. The tendency to the phase transitions discussed here is considerably weakened in the superconductors [1]. In the quasi-2D regime, the $4k_F$ CDW with alternate occupied sites is still possible. However, our demonstration that organic conductors have $V < V_c$ would explain the absence of this CDW transition. On the other hand, the absence of the BOW is a 2D effect. The BOW transition here is analogous to the spin Peierls transition in $\rho = 1$, which is weakened in 2D, and gives way to antiferromagnetism [17]. The CDW2 is a consequence of the BOWs and is thus also expected to vanish in 2D. The only remaining possible transition is then to the $2k_F$ SDW, and it has been argued [18] that for ρ away from 1 the SDW first requires a minimal 2D hopping, but then gradually weakens as the extent of two dimensionality increases. This would be supported by the occurrence of

a spin Peierls transition in the quasi-1D TMTTF materials, the occurrence of SDW in the weakly 2D TMTSF, its vanishing under pressure, and the absence of both spin Peierls and SDW transitions in the even more strongly 2D BEDT-TTF. Thus all possible spatial broken symmetries are considerably weakened in $\rho = 0.5$ in the quasi-2D regime for $V < V_c$. Whether or not superconductivity is related to the suppression of spatial broken symmetries is an intriguing question.

Some of these calculations were done on the iPSC/860 and Paragon at the San Diego Supercomputer Center. D.T. was supported by DOE Grant No. DE-FG02-85ER-40213.

-
- [1] See *The Physics and Chemistry of Organic Superconductors*, edited by G. Saito and S. Kagoshima (Springer-Verlag, Berlin, 1990).
 - [2] J.P. Pouget and R. Comes, in *Charge Density Waves in Solids*, edited by L.P. Gorkov and G. Gruner (North-Holland, Amsterdam, 1989), pp. 85–136, and references therein.
 - [3] V.J. Emery, in *Highly Conducting One-Dimensional Solids*, edited by J.T. Devreese *et al.* (Plenum, New York, 1979), p. 247.
 - [4] J.E. Hirsch and D.J. Scalapino, *Phys. Rev. Lett.* **50**, 1168 (1983); *Phys. Rev. B* **27**, 7169 (1983); **29**, 5554 (1984).
 - [5] S. Mazumdar, S.N. Dixit, and A.N. Bloch, *Phys. Rev. B* **30**, 4842 (1984).
 - [6] K.C. Ung, S. Mazumdar, and D.K. Campbell, *Solid State Commun.* **85**, 917 (1992).
 - [7] R.J.J. Visser, S. Oostra, C. Vettier, and J. Voiron, *Phys. Rev. B* **28**, 2074 (1983).
 - [8] H. Kobayashi, Y. Ohashi, F. Marumo, and Y. Saito, *Acta Crystallogr. Sect. B* **26**, 459 (1970).
 - [9] J. Hubbard, *Phys. Rev. B* **17**, 494 (1978).
 - [10] E.M. Conwell, A.J. Epstein, and M.J. Rice, in *Lecture Notes in Physics*, edited by S. Barisic and J.C. Cooper (Springer, Berlin, 1979), Vol. 95, p. 204; E.M. Conwell and I.A. Howard, *Phys. Rev. B* **31**, 7835 (1985).
 - [11] J. Kondo and K. Yamaji, *J. Phys. Soc. Jpn.* **43**, 424 (1977).
 - [12] M.J. Rice *et al.*, *Phys. Rev. B* **21**, 3437 (1980).
 - [13] R. Bozio and C. Pecile, in *Spectroscopy of Advanced Materials*, edited by R.J.H. Clark and R.E. Hester (Wiley, New York, 1991).
 - [14] P.P. Bendt, *Phys. Rev. B* **30**, 3951 (1984), and references therein.
 - [15] H.Q. Lin, E. Gagliano, D.K. Campbell, and J.E. Gubernatis (unpublished).
 - [16] S.N. Dixit and S. Mazumdar, *Phys. Rev. B* **29**, 1824 (1984).
 - [17] S. Mazumdar, *Phys. Rev. B* **36**, 7190 (1987); S. Tang and J.E. Hirsch, *Phys. Rev. B* **37**, 9546 (1988).
 - [18] S. Mazumdar, H.Q. Lin, and D.K. Campbell, *Synth. Met.* **41–43**, 4047 (1991).